

На основі теорії R -функцій розроблено нові підходи до аналітичної ідентифікації поверхонь безпілотних літальних апаратів (БПЛА) для реалізації технології 3D-друку.

Теорія R -функцій дозволяє описувати геометричні об'єкти складної форми єдиним аналітичним виразом, тобто, отримувати математичну модель об'єкта у вигляді рівняння. Для побудови таких рівнянь в роботі застосовано як добре відому методичку стандартних примітивів (шар, еліпсоїд, циліндр, конус, піраміда та ін.), так і новий підхід – блендінг на каркасі, який дозволяє будувати багатопараметричні рівняння із заданими властивостями. Побудовано та візуалізовано багатопараметричні рівняння поверхонь безпілотних літальних апаратів літакового типу різних форм та призначень. Адекватність отриманих результатів проєктованим об'єктам підтверджується візуалізацією як в умовах експлуатації програми RFPreview, так і реалізацією на 3D-принтері. Використання буквених параметрів при завданні геометричної інформації в аналітичному вигляді дозволяє оперативно змінювати розміри та форму проєктованих об'єктів, що допомагає скоротити витрати часу при побудові розрахункових моделей. Запропонований метод може скоротити трудомісткість робіт в САД-системах на місяці у тих випадках, коли потрібно переглянути велику кількість варіантів конструкції в пошуках оптимального розв'язку. Маючи рівняння об'єкту, можна легко отримати рівняння будь-якого його перерізу, що є корисним для числових розрахунків, а саме – при побудові різних цевих сіток.

Це може дати великий ефект зі зниження трудомісткості при побудові розрахункових моделей для визначення аерогазодинамічних та міцнісних характеристик. Визначення характеристик також часто пов'язане з необхідністю обліку зміни форми літального апарата. Це призводить до того, що визначення аеродинамічних характеристик тільки за рахунок необхідності побудови великої кількості розрахункових моделей для врахування цього фактору збільшує тривалість робіт на місяці. При параметричному завданні зміна розрахункових областей проводиться практично миттєво

Ключові слова: безпілотний літальний апарат, R -функції, 3D-принтер, стандартний примітив, блендінг на каркасі

UDC 517.95+518.517+629.735.33-519

DOI: 10.15587/1729-4061.2019.155548

ANALYTICAL IDENTIFICATION OF THE UNMANNED AERIAL VEHICLES' SURFACES FOR THE IMPLEMENTATION AT A 3D PRINTER

T. Sheyko

Doctor of Technical Sciences, Professor
Department of Mathematical Modeling
and Optimal Design*

E-mail: sheyko@ipmach.kharkov.ua

K. Maksymenko-Sheyko

Doctor of Technical Sciences, Senior Researcher*

Professor

Department of Information Technology in
Physics and Energy Systems

V. N. Karazin Kharkiv National University
Svobody sq., 4, Kharkiv, Ukraine, 61022

E-mail: m-sh@ipmach.kharkov.ua

V. Sirenko

PhD

Deputy Chief Designer for System Design of Missiles
and Missile Systems – Head of the theoretical design
complex for design and calculations in terms of ballistics,
aerodynamics, heat and mass transfer, strength

Yuzhnoye State Design Office

Kryvoriz'ka str., 3, Dnipro, Ukraine, 49008

E-mail: v.n.sirenko@i.ua

A. Morozova

Senior Lecturer

Department of Systems Engineering**

R. Petrova

PhD

Department of Economic Cybernetics and
Management of Economic Security**

E-mail: roksana.petrova@nure.ua

*A. N. Podgorny Institute for Mechanical Engineering
Problems of NAS of Ukraine

Pozharskoho str., 2/10, Kharkiv, Ukraine, 61046

**Kharkiv National University of Radio Electronics

Nauky ave., 14, Kharkiv, Ukraine, 61166

1. Introduction

Drones (unmanned aerial vehicles) are becoming increasingly popular all over the world every day. This is

due to a series of advantages over manned aircraft, namely, absence of crew, relatively low cost of the drone at a long duration and large range of flight. Design characteristics of drones differ which diversifies areas of their application.

Unlike light, heavy drones are mainly involved in hostilities for executing intelligence operations or destroying concrete targets. Drones are endowed with many positive qualities. Preservation of the pilot's life is the most important of these qualities. Civilian and commercial use of drones is not yet well developed although the area of potential use of drones is very extensive. It includes delivery of goods, monitoring of environment and forest fires, border patrolling, prevention of drug smuggling, aerial reconnaissance and mapping, traffic control, etc. By their types, drones are divided into plane, helicopter and convertiplane classes. From time to time, the military, officers of the Ministry of Emergency Situation and research scientists get into a situation when it is necessary to carry out reconnaissance of inaccessible areas or detect location of a specific object. Such tasks can be dangerous to human life and health, so they are entrusted to light drones today. Experts are confident that the basic technical problems in creating modern drones include fundamental development of artificial intelligence systems as well as drone designs, shapes and motors, aerodynamics study, etc. [1–4].

Three-dimensional (3D) printing is one of the new technologies gaining growing popularity at present. 3D printing allows one to create three-dimensional models of any objects using special equipment: a 3D printer. Advantages of using modern 3D printers include reduction of cost of the product manufacture and the time in which the product enters the market, modeling objects of any shape and complexity, high speed and precision of manufacture and freedom of material choice.

NASA engineers are building a rocket from a special plastic capable of reaching other planets in the solar system using a 3D printer with a technology of selective laser sintering. Students at Southampton University have created the world's first aircraft called Sulsa (Southampton University Laser Sintered Aircraft) with the use of a 3D printer [5] and the British Navy got down to using it for ice reconnaissance in Antarctica [6].

Airbus Company has presented at the Berlin Air Show a drone of Thor model printed on a 3D printer [7]. Its length is about 4 meters, the wingspan is the same. The device weighs about 25 kg. The company explains that the new drone was developed for aerodynamic studies associated with high risk, hence the use of 3D printing was preferred as it makes it possible to create the device in several weeks and at much lower costs.

The drone, however, is not the only Airbus innovation having connection with 3D printing. The company also carries out aerodynamic tests of wing sections printed with a 3D printer. In this case, 3D printing reduces production time by 90 % and costs by 75 %. Besides, Airbus plans installation of partitions separating passenger cabin from kitchen printed with a 3D-printer. Due to the design features and owing to 3D printing, the partition will be 50 % lighter.

The given examples indicate that creation of both models and actual drones with the use of 3D printers is a promising project. Therefore, it is necessary to develop appropriate hardware support in a form of high-tech computer systems based on the most advanced achievements of the present-day mathematics.

2. Literature review and problem statement

Designing drones and control systems for them cannot be imagined without mathematical simulation of drone

flight. The modern approach to designing involves creation of models that best of all reflect properties and behavioral patterns of real drones. Many tasks of using drones that are posed before researchers can be solved at the design stage. Major technical potential has been created in a form of high-speed computers and advanced software to create mathematical models, e. g. such software packages as Solid Works, Ansys CFX, POLYE, etc. In all software systems, the problem of geometry data setting arises and is solved in different ways to create a mathematical and computer model of the drone being designed. For example, the wing cross section profile is specified in [9] by standard Ansys modeling tools entailing building of a new model at any slightest change of the profile appearance. NASA standard wing profiles specified point-by-point are used in [10]. In addition, TsAGI standard profiles are used in [11].

Numerical CFD methods of the LES type as well as panel methods and the method of discrete vortexes are used in [12] for aerodynamic analysis and then, based on the results, changes are introduced to the aircraft shape. In essence, this is how the inverse problem is solved.

The authors of [13] took advantage of an existing drone for their studies. However, this drone was designed for a common use. Presumably, if the authors could introduce changes to the shape of the drone surface, the study would be more effective.

Study [14] is devoted to correction for wind effect on the drone flight. A special control algorithm was proposed for such correction. However, this algorithm would probably be simpler if the wind effect was taken into consideration during the drone design stage. To this end, one can change its shape to make the flight more stable.

To compile component equations of a complicated system of a drone complex, the theory of dynamic systems of randomly changing structures most fully reflecting the random stick-slip nature of impacts to which the system is exposed was used in [15]. To reduce the degree of impact randomness, it is necessary to correct shape of the drone surface. This will make the drone flight steadier.

The examples show that shape of the drone surface is essential in all studies and requires constant adjustment when dealing with it. Any slightest change in appearance of the surface shape in the considered methods and approaches entails construction of a new model while insufficient attention is paid to parametric specification of the drone surfaces. Developers must be skilled in building mathematical models of surfaces which will respond promptly to changes in shape of the object under study.

Calculations and tests of a new aircraft should be given considerable attention. It should be noted that 3D printing can be of great help in this. There are different approaches to creation of 3D models depending on the data being set for printing:

1. 3D scanning of an existing object.
2. Construction of a 3D model using a rather wide range of software products that have primitive forms of various types in the arsenal of their libraries.
3. Creation of a 3D-model with the help of the mathematical apparatus of analytical geometry.

In cases when the modeled object exists physically, use of a 3D scanner is the most convenient way of obtaining 3D models. However, in the case when the modeled object has impressive dimensions or does not exist at all, this approach is inapplicable. In such cases, creation of 3D models can be

realized using software products. However, this method also has a series of drawbacks, namely lack of a history of model construction, limited set of primitives in the library program modules, lack of possibility of analytical record, etc.

One of the ways for solving this problem is application of the R-functions theory, which allows one to describe geometric objects of a complex shape with a single analytical expression [16–18] which necessitates conducting studies in this direction.

3. The aim and objectives of the study

This study objective was creation of mathematical and computer models of a series of drones based on the R-functions theory for realization of the 3D printing technology.

To attain this objective, it was necessary to solve the following tasks:

- explore mathematical apparatus of the R-functions theory and its application to creation of multiparameter equations of the three-dimensional drone surfaces and their realization on a 3D printer;
- develop an algorithm of phased construction of the drone surface equations;
- explore possibilities of using both the well-known procedure of standard primitives and blending on a frame for constructing multiparameter equations of drone surfaces and realization on a 3D printer;
- realize the constructed mathematical model of a drone on a 3D printer.

4. The study materials and methods

4. 1. Engineering environment of the R-functions theory

When constructing mathematical models using the R-function method, both simplest R-operations [16–18]

$$fk \wedge_0 fl = fk + fl - \sqrt{fk^2 + fl^2};$$

$$fk \vee_0 fl = fk + fl + \sqrt{fk^2 + fl^2},$$

and R-operations for smoothing sharp edges and corners were used [17]:

$$fk \wedge_\rho fl = fk + fl - \sqrt{fk^2 + fl^2 + \frac{FR}{8\rho^2}(|FR + FR|)};$$

$$fk \vee_\rho fl = fk + fl + \sqrt{fk^2 + fl^2 + \frac{FR}{8\rho^2}(|FR + FR|)},$$

where

$$FR = \rho^2 - fk^2 - fl^2.$$

Both well-known procedure of standard primitives [16, 17] and the new approach, blending on a frame, were used. To guide the reader’s eye, let us first consider the case when the frame is a line segment.

$$fi1 = \frac{a^2 - x^2}{2a} \geq 0; \quad f11 = \sqrt{y^2 + z^2};$$

$$fff1 = \sqrt{\left(0.5\sqrt{f11^4 + fi1^2} - fi1\right)^2 + f11^2} \geq 0;$$

$$\omega = -fff1 + \frac{(a1-x)(a2+x)}{p1} + p2 \geq 0.$$

As a result, we obtain a body of rotation (Fig. 1, a) and four controlled parameters. Consider also the case when the frame is a circle arc.

$$f1 = \frac{R^2 - (x+R)^2 - y^2}{2R} \geq 0;$$

$$fi = \frac{y+x+R}{\sqrt{2}} \wedge_0 \frac{-y+x+R}{\sqrt{2}} \geq 0;$$

$$fff1 = \sqrt{\left(0.5\sqrt{f1^4 + fi^2} - fi\right)^2 + f1^2} \geq 0;$$

$$\omega = -ff1^2 + \left[\frac{(a1+y)(a2-y)}{par1} - par2 \right]^2 \geq 0.$$

As a result, we obtain a cylindrical body (Fig. 1, b) with a guide similar to the Zhukovsky profile and four controlled parameters.

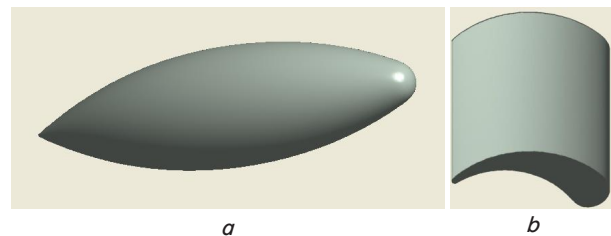


Fig. 1. Surfaces constructed using the method of blending on a frame : body of rotation (a); cylindrical body with a guide similar to the Zhukovsky profile (b)

It should be noted that in this case, the use of R-operations and full normalization to the first order of functions, *fff1*, [10] has made it possible to realize the procedure of blending on a frame.

4. 2. 3D printing based on the technology of fused deposition modeling (FDM)

In order to print an object on a 3D printer, it is necessary to model it and prepare for printing. The software packages enabling creation of the three-dimensional graphics, that is, simulate objects of virtual reality and create images on the basis of these models vary greatly. In this study, we used the RFPReview program which allowed us to save the object model in a STL format. It was necessary to prepare it for layered printing (generate a G-code). The software that performs this conversion is called a slicer. The slicer allows one to see how a model is positioned on a 3D printer platform before printing, whether supports are necessary for structural elements, select all printing parameters and settings. In this study, the authors used the Cura slicer to generate G-code for 3D printers. The program has a wide selection of settings and plug-ins. With the help of Cura, one can dynamically change temperature during printing, printout objects with fine details, etc.

The technology of 3D printing is based on the technology of layer-by-layer “growing” solid objects from various materials. The FDM technology is a prototyping method using industrial grade thermoplasts.

5. Results of analytical identification of drone surfaces

A mathematical and computer model of the drone mock-up shown in Fig. 2 was constructed. For this purpose, we used both the method of blending on a frame and known equations of standard primitives, namely, equations of cylinder, triangular pyramid and ellipsoid.

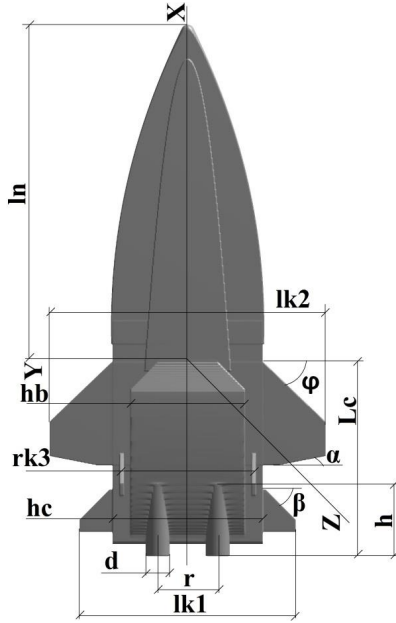


Fig. 2. Schematic drone mock-up

The main body.

$$fi1 = \frac{a^2 - x^2}{2a} \geq 0; f11 = \sqrt{y^2 + z^2};$$

$$fff1 = \sqrt{(0.5\sqrt{f11^4 + fi1^2} - fi1)^2 + f11^2};$$

$$\omega p = -fff1 + \frac{(a1-x)(a2+x)}{p1} + p2;$$

$$\omega n = (\omega p \wedge_0 \delta^2 - z^2) \wedge_0 x + l1 \geq 0;$$

$$\omega c1 = \left(\left(\left(\left(1 - \frac{z^2}{oz^2} - \frac{(x+1)^2}{ox^2} \right) \wedge_0 \right) \wedge_0 (\delta - z) \right) \wedge_0 -xtg\lambda + z \geq 0; \right. \\ \left. \wedge_0 \left(1.25^2 - \frac{y^2}{oy^2} \right) \right)$$

$$\omega c2 = \left(\left(\left(\left(\left(1 - \frac{z^2}{ozn^2} - \frac{(x+1)^2}{oxn^2} \right) \wedge_0 \right) \wedge_0 \left(\frac{\delta}{2} + z \right) \right) \wedge_0 (-x - 2\delta) \right) \wedge_0 -xtg\lambda - z \geq 0; \right.$$

$$\omega c3 = \omega c2 \wedge_0 (x^2 - y^2) \geq 0;$$

$$\omega c = (\omega c1 \wedge_0 (hc + z)) \vee_0 \omega c3 \geq 0;$$

$$\omega d = \left(\left(\left(\frac{d^2}{4} - \left(y - \frac{lk1}{2} \right)^2 - (z - hz)^2 \right) \vee_0 \right) \wedge_0 (x + Lc)(-x - Lc + h) \geq 0; \right. \\ \left. \vee_0 \left(\frac{d^2}{4} - \left(y + \frac{lk1}{2} \right)^2 - (z - hz)^2 \right) \right)$$

$$\omega 1 = \omega n \vee_0 \omega c \geq 0;$$

$$\omega n1 = ((-x + x0 - ky^2) \wedge_0 (x + xnak)) \wedge_0 z(hnak - z) \geq 0$$

– overlay on the nose,

$$\omega \omega n = ((ab/2)^2 - y^2) \wedge_0 (z - hb) \wedge_0 (lb - x) \geq 0$$

– cutout in the underbelly,

$$rak1 = (rsh^2 - (x + xhr)^2 - y^2 - (z + zr)^2) \vee_0$$

$$\vee_0 (rsh^2 - (x - xhr)^2 - y^2 - (z + zr)^2) \geq 0;$$

$$rak = \left(\left(rsh^2 - y^2 - (z + zr)^2 \right) \wedge_0 \right) \vee_0 rak1 \geq 0 \\ \wedge_0 ((xhr + x)(xnr - x))$$

– rocket body with rounded ends,

$$\omega kor = (((\omega 1 \vee_0 \omega d) \vee_0 \omega n1) \wedge_0 -\omega \omega n) \vee_0 rak \geq 0$$

– main body.

The fairing in front of the rocket in the underbelly

$$y1 = -\frac{cpx \cdot y}{x - xpn - cpx};$$

$$z1 = -\frac{cpx \cdot z}{x - xpn - cpx};$$

$$\omega nizp = \left(\left((z1 + zo)(zon - z1) \right) \wedge_0 \right) \wedge_0 ((xp - x)(x - xpn)) \geq 0 \\ \wedge_0 (-4y^2 + (z1 + zo)^2)$$

– triangular pyramid

$$\omega niz1 = ((z + zo)(zon - z)) \wedge_0 (-ko \cdot y^2 + (z + zo)^2) \geq 0;$$

$$\omega nizz = \omega niz1 \vee_0 (lob - x) \geq 0;$$

$$\omega niz = (\omega nizz \wedge_0 (x - 0.2 + z)) \vee_0 \omega nizp \geq 0 \text{ – fairing.}$$

Wings

$$\omega kr11 = \left(\left(\left(\delta - |z + \delta / 2| \right) \wedge_0 \right) \wedge_0 ((xnm + x)(-x - xbm - x)) \right) \wedge_0 \\ \wedge_0 (lk1^2 - y^2) \geq 0;$$

$$\omega kr1 = \omega kr11 \wedge_0 ((-x0c - x)^2 - y^2) \geq 0$$

– small horizontal wings,

$$\omega_{kr22} = \left(\begin{array}{l} (\delta - |z - \delta / 2|) \wedge_0 \\ \wedge_0 ((xnb + x)(-xbb - x)) \end{array} \right) \wedge_0 (lk2^2 - y^2) \geq 0;$$

$$\omega_{kr2} = \left(\omega_{kr22} \wedge_0 ((x00 - x)^2 - kkn y^2) \right) \wedge_0 \wedge_0 (-y^2 + kk1(-x01 - x)^2) \geq 0$$

– large horizontal wings,

$$\omega_{kr33} = \left(\left(\delta - |y^2 - (rk3 / 2)^2| \right) \wedge_0 (z(hz - z)) \right) \wedge_0 \wedge_0 ((x11 + x)(-x22 - x)) \geq 0;$$

$$\omega_{kr3} = \omega_{kr33} \wedge_0 ((xx1 + x)^2 - z^2) \geq 0$$

– vertical wings (stabilizers),

$$\omega_{kr} = \omega_{kr1} \vee_0 \omega_{kr2} \vee_0 \omega_{kr3} \geq 0 \text{ – assembly of wings.}$$

$$W = \omega_{kor} \vee_0 \omega_{kr} \vee_0 \omega_{niz} \geq 0$$

– complete assembly of the drone presented in Fig. 3.

```
n=1;a=5*n;
fi1=(a^2-x^2)/a;
f11=sqrt(y^2+z^2);
fff1=sqrt(((sqrt(f11^4+fi1^2)-fi1)/2)^2+f11^2);
p1=20*n;p2=0;a1=5.2*n;a2=5*n;
wp=-fff1+(a1-x)*(a2+x)/p1+p2;
wn=rfAND(rfAND(wp,(0.1*n)^2-z*z),x+0.2*n);
wc1=rfAND(rfAND(rfAND(1-z^2/(0.6*n)^2-(x+1*n)^2/(2.5*n)^2,(1.25*n)^2-y^2),0.1*n-z),-0.5*x+z);
wc2=rfAND(rfAND(rfAND(rfAND(1-z^2/(0.3*n)^2-(x+1*n)^2/(2.5*n)^2,(0.95*n)^2-y^2),0.05*n+z),-x-0.2*n),-0.3*x-z);
wc3=rfAND(wc2,x^2-y^2);
wc=rfOR(rfAND(wc1,0.5*n+z),wc3);
wd=rfAND(rfOR((0.2*n)^2-(y-0.5*n)^2-(z-0.05*n)^2,(0.2*n)^2-(y+0.5*n)^2-(z-0.05*n)^2),(x+4*n)*(-x-2.5*n));
w1=rfOR(wn,wc);
wn1=rfAND(rfAND(-x+4.5*n-10*n*y^2,x+0.65*n),z*(0.15*n-z));
wwn=rfAND(rfAND((0.21*n)^2-y^2,-z-0.01*n),2*n-x);
rak1=rfOR((0.2*n)^2-(x+2.9*n)^2-y^2-(z+0.21*n)^2,(0.2*n)^2-(x-0.3*n)^2-y^2-(z+0.21*n)^2);
rak=rfOR(rfAND((0.2*n)^2-y^2-(z+0.21*n)^2,(2.9*n+x)*(0.3*n-x)),rak1);
y1=-0.8*n*y/(x-2.2*n-0.8*n);z1=-0.8*n*z/(x-2.2*n-0.8*n);
wnizp=rfAND(rfAND((z1+0.6*n)*(0.1*n-z1),-4*n*y1^2+(z1+0.6*n)^2),(3*n-x)*(x-2.2*n));
wniz1=rfAND((z+0.6*n)*(0.1*n-z),-4*n*y^2+(z+0.6*n)^2);
wnizz=rfAND(wniz1,2.2*n-x);
wniz=rfOR(rfAND(wnizz,x-0.2*n+z),wnizp);
wkor=rfOR(rfAND(rfOR(rfOR(w1,wd),wn1),-wwn),rak);
wkr11=rfAND(rfAND(0.05*n-abs(z+0.05*n),(3.3*n+x)*(-2.6*n-x)),(1.8*n)^2-y^2);
wkr1=rfAND(wkr11,(-1.3*n-x)^2-y^2);
wkr22=rfAND(rfAND(0.05*n-abs(z-0.05*n),(2.2*n+x)*(-0.5*n-x)),(2.3*n)^2-y^2);
wkr2=rfAND(rfAND(wkr22,(0.7*n-x)^2-0.9*n*y^2),-y^2+26*n*(-2.5*n-x)^2);
wkr33=rfAND(rfAND(0.07*n-abs(y^2-(1.1*n)^2),z*(0.6*n-z)),(2.7*n+x)*(-2*n-x));
wkr3=rfAND(wkr33,(1.9*n+x)^2-z^2);
wkr=rfOR(rfOR(wkr1,wkr2),wkr3);
wfin1=rfOR(rfOR(wkor,wkr),wniz);
wfin=rfAND(wfin1,x+3.7*n);
niz=rfAND(1-y*y/(2.5*n)^2-z*z/(n^2),(x+3.8*n)*(-3.5*n-x));
%res=rfOR(wfin,niz);
res=wfin;
```

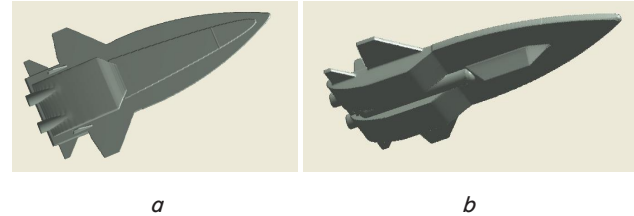


Fig. 3. A drone with a rocket: top view (a); bottom view (b)

The results presented in Fig. 3 were obtained for the following values of literal parameters: $a=5$; $p1=20$; $p2=0$; $a1=5.2$; $a2=5$; $\delta=0.1$; $l1=0.2$; $lk1=1$; $hz=0.05$; $Lc=4$; $h=1.5$; $lk1=1.8$; $lk2=2.3$; $rsh=0.2$; $oz=0.6$; $ox=2.5$; $oy=1$; $tg\lambda=0.5$; $ozn=0.3$; $oxn=2.5$; $oyn=1$; $tg\lambda1=0.3$; $he=0.5$; $hnak=0.15$; $x0=4.5$; $k=10$; $xnak=0.65$; $ab/2=0.21$; $hb=0.01$; $lb=2$; $zr=0.21$; $xhr=2.9$; $xnr=0.3$; $lob=2.2$; $xnm=3.3$; $xbm=2.6$; $xnb=2.2$; $xbb=0.5$; $x0c=1.3$; $hz=0.6$; $x11=2.7$; $x22=2$; $x00=0.7$; $kk=0.9$; $kk1=26$; $fk12=fk1 \vee_0 fk2 \geq 0$; $\omega c = fk12 \vee_0 fc \geq 0$; $x01=2.5$; $xx1=1.9$; $ko=4$; $zo=0.6$; $zon=0.1$; $apy=0$; $bpz=0$; $cpx=0.8$; $xp=3$; $xpn=2.2$.

To carry out experimental realization of the model of the constructed drone, the RFPReview software package [18] based on the R-functions theory with literal parameters was used. It has allowed us to write the following program and obtain an stl file for subsequent 3D printer operation.

As a result of work of the program and the 3D printer, the model shown in Fig. 4 was obtained.

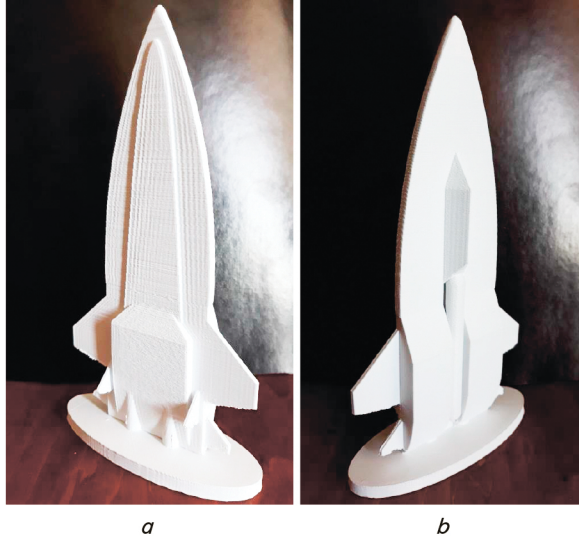


Fig. 4. The mock-up of the drone printed at a 3D-printer: top view (a); bottom view (b)

It should be noted that with the change of any of the 55 presented literal parameters, shapes of corresponding drone fragments will be automatically changed.

Equation of the product shown in Fig. 4 was derived. To derive the fuselage equation, known equations of standard primitives were used, namely, the equation of cylinder and the equations of two conical surfaces.

Fuselage.

$$f1 = \frac{R^2 - xc_1^2 - z^2}{2R} \geq 0; \quad f2 = \frac{a^2 - yc_1}{2a} \geq 0;$$

$$fc = f1 \wedge_0 f2 \geq 0;$$

where

$$xc_1 = x \frac{\sqrt{2}}{2} - y \frac{\sqrt{2}}{2};$$

$$yc_1 = x \frac{\sqrt{2}}{2} + y \frac{\sqrt{2}}{2};$$

$$fk11 = \frac{R^2 - x_1^2 - z_1^2}{2R} \wedge_0 \frac{(a - y01 + yc_1)(-a - yc_1)}{|y01|} \geq 0;$$

$$fk1 = fk11 \wedge_0 (a - y01 - cv + yc_1) \geq 0,$$

where

$$x_1 = x01 - y01 \frac{xc_1 - x01}{yc_1 + a - y01};$$

$$z_1 = z01 - y01 \frac{z - z01}{yc_1 + a - y01};$$

$$fk2 = \frac{R^2 - x_2^2 - z_2^2}{2R} \wedge_0 \frac{(a + y02 + yc_1)(yc_1 - a)}{|y02|} \geq 0,$$

where

$$x_2 = x02 - y02 \frac{xc_1 - x02}{yc_1 - a - y02};$$

$$z_2 = z02 - y02 \frac{z - z02}{yc_1 - a - y02};$$

$$\omega cam = \omega 2kr \vee_p \omega c \geq 0, \quad \rho = r1s.$$

Derivations were made with the following values of literal parameters:

$$a = 10; \quad R = 3.5;$$

$$x01 = 0; \quad y01 = -15; \quad z01 = 2.2;$$

$$x02 = 0; \quad y02 = 10; \quad z02 = -R;$$

$$cv = 4; \quad r1s = 2.$$

Two variants of wing structures were considered: with the use of standard primitives and R-operations for smoothing sharp edges as well as blending on a frame in a form of a circle arc.

Variant 1. The right wing.

$$f1 = \frac{-z_1 + 0.1x}{\sqrt{1.01}} \geq 0;$$

$$f2 = \frac{z_1 + 0.1x}{\sqrt{1.01}} \geq 0;$$

$$f3 = 7 - x \geq 0;$$

$$z_1 = z + 2.5;$$

$$f4 = \frac{(3 - y)(17 + y)}{20} \geq 0;$$

$$\omega 1 = f1 \wedge_p f2 \geq 0, \quad \rho = r1 = 0.3;$$

$$\omega k = \omega 1 \wedge_p f3 \geq 0, \quad \rho = r2 = 0.5;$$

$$\omega \omega = \omega k \wedge_p f4 \geq 0, \quad \rho = r3 = 0.5.$$

The left wing.

$$xp = y; \quad yp = x; \quad zp = z;$$

$$f1p = \frac{-zp + 0.1xp}{\sqrt{1.01}} \geq 0; \quad f2p = \frac{zp + 0.1xp}{\sqrt{1.01}} \geq 0;$$

$$f3p = 7 - xp \geq 0;$$

$$f4p = \frac{(3 - yp)(17 + yp)}{20} \geq 0;$$

$$\omega 1p = f1p \wedge_p f2p \geq 0, \quad \rho = r1 = 0.3;$$

$$\omega kp = \omega 1p \wedge_p f3p \geq 0, \quad \rho = r2 = 0.5;$$

$$\omega \omega p = \omega kp \wedge_p f4p \geq 0,$$

$$\rho = r3 = 0.5; \quad \omega 2kr = \omega \omega \vee_0 \omega \omega p \geq 0$$

– two wings.

Variant 2. *The right wing.*

$$z1=z; rk=6;$$

$$f1 = \frac{rk^2 - (z_1 + rk)^2 - y^2}{2rk} \geq 0;$$

$$fi = \frac{y + z_1 + rk}{\sqrt{2}} \wedge_0 \frac{-y + z_1 + rk}{\sqrt{2}} \geq 0;$$

$$ff1 = \sqrt{\left(0.5\sqrt{f1^4 + fi^2} - fi\right)^2 + f1^2};$$

$$tt = \frac{(20 + y)(1.2 - y)}{par1} - par2;$$

$$par1 = 300; par2 = 0.4;$$

$$\omega l = tt^2 - ff1^2;$$

$$\omega k = \omega l \wedge_0 (1 - x)(17 + x) \geq 0; \omega \omega = \omega k \wedge_0 y - 4x + 2 \geq 0.$$

The left wing.

$$xp = y; yp = x; zp = z_1;$$

$$f1p = \frac{rk^2 - (zp + rk)^2 - yp^2}{2rk} \geq 0;$$

$$fip = \frac{yp + zp + rk}{\sqrt{2}} \wedge_0 \frac{-yp + zp + rk}{\sqrt{2}} \geq 0;$$

$$ff1p = \sqrt{\left(0.5\sqrt{f1p^4 + fip^2} - fip\right)^2 + f1p^2};$$

$$tpp = \frac{(20 + yp)(1.2 - yp)}{par1} - par2;$$

$$par1 = 300; par2 = 0.4;$$

$$\omega lp = tpp^2 - ff1p^2;$$

$$\omega kp = \omega lp \wedge_0 (1 - xp)(17 + xp) \geq 0;$$

$$\omega \omega p = \omega kp \wedge_0 yp - 4xp + 2 \geq 0;$$

$$\omega 2kr = \omega \omega \vee_0 \omega \omega p \geq 0.$$

The tail assembly.

$$\omega f1 = \frac{-z - 2(y c_1 + 7)}{\sqrt{5}} \wedge_0 \frac{z + 2(y c_1 + 17)}{\sqrt{5}} \geq 0;$$

$$\omega f = \left(\omega f1 \wedge_0 \frac{0.3^2 - xc_1^2}{0.6} \right) \wedge_0 \frac{z(8 - z)}{8} \geq 0.$$

Finally, the following is obtained:

$$W = \omega f \wedge_0 \omega cam \geq 0, \rho = rxs = 2.$$

The model of the drone with wings constructed according to the first variant is presented in Fig. 5, a, and that for the second variant is presented in Fig. 5, b.

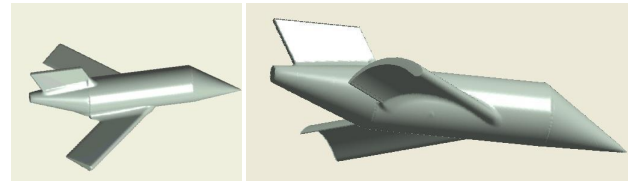


Fig. 5. Drones with different wing profiles: with the use of standard primitives and R-operations for smoothing sharp edges (a); with the use of blending on a frame in a form of a circle arc (b)

The ten-parameter equation of the drone fuselage with two different multiparameter equations of the wing profile derived using standard primitives makes it possible to promptly change the drone shape when values of the literal parameters change.

A fuselage equation was derived using blending on frames in a form of straight line segments of which one had $2a$ length and the other had $2b$ length and was shifted to the nose by xc after which they were combined using R-disjunctions.

$$x_1 = x \frac{\sqrt{2}}{2} + y \frac{\sqrt{2}}{2}; y_1 = -x \frac{\sqrt{2}}{2} + y \frac{\sqrt{2}}{2};$$

$$fi1 = \frac{a^2 - x1^2}{2a} \geq 0;$$

$$f11 = \sqrt{y1^2 + z^2};$$

$$ff1 = \sqrt{\left(\left(\left(\sqrt{f11^4 + fi1^2}\right) - fi1\right) / 2\right)^2 + f11^2} \geq 0;$$

$$\omega p = (ff1 + (a1 - x1)(a2 + x1) / p1 + p2) \wedge_0 \wedge_0 (2.5^2 - z^2 - y1^2) \geq 0;$$

$$fib1 = \frac{b^2 - (x1 - xc)^2}{2b} \geq 0;$$

$$fb11 = \sqrt{y1^2 + (z - 0.5)^2};$$

$$fffb1 = \sqrt{\left(\left(\left(\sqrt{fb11^4 + fib1^2}\right) - fib1\right) / 2\right)^2 + fb11^2} \geq 0;$$

$$\omega pb = fffb1 + (ba1 - x1 + xc)(ba2 + x1 - xc) / pb1 + pb2 \geq 0;$$

$$\omega c = \omega p \vee_0 \omega pb \geq 0;$$

$$W = \omega 2k \vee_0 \omega c \geq 0.$$

Parameters:

$$a = 15; p1 = 60; p2 = 0; a1 = 15; a2 = 16; b = 4;$$

$$xc = 7; pb1 = 8; pb2 = 0; ba1 = 7; ba2 = 4.$$

Drone mock-ups for different values of literal P1 parameter are shown in Fig. 6.

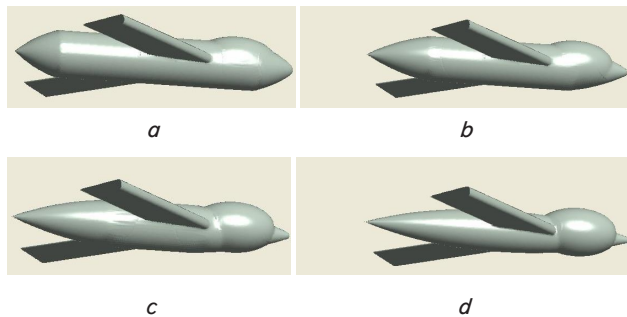


Fig. 6. Drones designed for obtaining intelligence information and its delivery to destination: $p_1=40$ (a); $p_1=60$ (b); $p_1=80$ (c); $p_1=100$ (d)

Thus, value of the p_1 parameter significantly affects appearance of the tail and head parts of the fuselage.

Fig. 7 shows effect of value of the p_2 parameter on appearance of the drone surface.

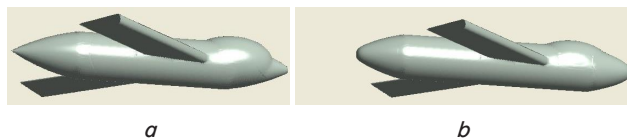


Fig. 7. Influence of values of the literal parameters on appearance of the drone surface: $p_1=60, p_2=0$ (a), $p_1=60, p_2=1$ (b)

Thus, the p_2 parameter affects smoothing of the tail and head parts of the fuselage.

The resulting equations of object models were visualized using the RFPReview program [18].

6. Discussion of results obtained in the analytical identification of drone surfaces

Construction of mathematical models of objects is an important issue in realization of 3D printing. In this study, it is creation of a 3D model using the mathematical apparatus of analytical geometry, respectively. The R-functions theory solves the inverse problem of analytical geometry allowing one to describe geometric objects of a complex shape with a single analytical expression. Summing up, it should be noted that thanks to the R-functions theory, equations of surfaces of a drone of a plane type were derived in this study. They have form of general analytical expressions with literal parameters applicable both in solving strength and aerodynamic problems and in designing and manufacturing products (in this case, by means of a 3D-printer). The use of literal parameters enables quick change of characteristic dimensions and shape of the object under study. The feature of positiveness of the constructed function in internal points of the object is very convenient for realization of 3D printing. Having equation of an object, one can easily obtain equation of its any cross section which is useful in numerical calculations using CFD-methods (e. g. [19]), namely, when constructing computational meshes.

We used both the well-known procedure of standard primitives (sphere, ellipsoid, cylinder, cone, pyramid, etc.) as well as the new approach, blending on a frame, which makes it possible to derive multiparameter equations with desired properties. Wings and experimental fuselage of the drone were built in this way.

As disadvantages, it is necessary that the engineering researcher shall be skilled in the mathematical apparatus of the R-functions theory and a limited set of standard primitives in library modules of the programs aimed at using the R-functions theory. The authors are planning to implement automation of the process of deriving equations of a drone of a plane type composed from standard primitives which will make the derivation process more accessible to the user. Also, further development of this procedure in relation to drones of helicopter and convertiplane types is planned.

The proposed method of specifying the shape of products using a limited number of parameters can significantly reduce complexity of work in CAD systems in cases when it is necessary to view a large number of design variants in a search for an optimal solution. This can have a great effect on reducing complexity in construction of computational models for determining aero-gas-dynamic and strength characteristics. For example, the process of building a perturbed flow region around an aircraft of a complex shape can take from several working days to weeks. At the same time, successive review of a large number of structure design variants is required during the design process in order to optimize the structure characteristics. Following deciding on the aircraft shape, characterization is also often associated with the need to take into consideration changes in the aircraft shape, e.g. if it has controls that change shape in the flight. This leads to a situation when defining aerodynamic characteristics, just the need of building a large number of computational models to account for this factor extends the work duration for months. The change in rated operating conditions is almost instantaneous in parameter specification.

7. Conclusions

1. Mathematical apparatus of the R-functions theory which has hitherto been used mainly in 2D problems has been studied. It has also appeared to be effective when applied in 3D problems as it was demonstrated by the visualized equations and the models fabricated on a 3D printer.

2. An algorithm of phased construction of drone equations has been developed and implemented with the help of R-functions which makes it possible to check and introduce adjustments to the model at each stage of its construction.

3. The method of standard primitives can only be used in the case of completeness of the base of standard primitives. Otherwise, it is necessary to develop methods for constructing surfaces based on other approaches. Blending on a frame used in the study can be considered as one of possible approaches.

4. The constructed mathematical model of the drone was realized on the Anet A8 3D printer working with the use of the FDM technology. The use of other, more advanced technologies of 3D printing will improve appearance of products.

References

1. UAV Classification and Intelligent Management Systems / Fedorov S. I., Haustov A. V., Kramarenko T. M., Dolgih V. S. // Otkrytye informacionnye i komp'yuternye integrirovannye tekhnologii. 2016. Issue 74. P. 12–21.

2. Austin R. Unmanned Aircraft Systems: UAVS Design, Development and Deployment. John Wiley and Sons, 2010. 332 p. doi: <https://doi.org/10.1002/9780470664797>
3. Arjomandi M. Classification of Unmanned Aerial Vehicles // MECH ENG 3016. Aeronautical Engineering. The University of Adelaide Australia, 2006. 49 p.
4. Unmanned Aircraft System Operation in UK. Airspace – Guidance: CAP 722. Civil Aviation Authority, 2010. 96 p.
5. Salsa – perviy v mire samolet, napechatanniy na printere. URL: <http://www.novate.ru/blogs/030811/18344/>
6. Napechatanniy na 3D-printere samolet prinyat na sluzhbu v Antarktide. URL: <https://3dnews.ru/931573>
7. AIRBUS predstavlyaet THOR – napechatanniy na 3D-printere bespilotnik. URL: <http://www.3dpulse.ru/news/promyshlennost/airbus-predstavlyaet-thor-napechatanniy-na-3d-printere-bespilotnik/>
8. Napechatanniy na 3D-printere rossiyskiy bespilotnik pokazali na “Innoprome”. URL: <http://www.interfax.ru/russia/517842>
9. Prisacariu V. CFD Analysis of UAV Flying Wing // INCAS BULLETIN. 2016. Vol. 8, Issue 3. P. 65–72. doi: <https://doi.org/10.13111/2066-8201.2016.8.3.6>
10. Static aeroelastic analysis including geometric nonlinearities based on reduced order model / Xie C., An C., Liu Y., Yang C. // Chinese Journal of Aeronautics. 2017. Vol. 30, Issue 2. P. 638–650. doi: <https://doi.org/10.1016/j.cja.2016.12.031>
11. Pogrebnaya T. V., Shipilov S. D. Method for numerical modeling of unsteady separated flow around airfoils moving close to flat screen // Nauchniy vestnik Moskovskogo gosudarstvennogo tekhnicheskogo universiteta grazhdanskoy aviatsii. 2017. Vol. 20, Issue 2. P. 46–56.
12. Bulat P. V., Minin O. P. On modern approach to airplane-type unmanned aerial vehicles design with short takeoff and landing. Part III. Numerical modeling of aircraft vortex aerodynamics by discrete vortex method // Scientific and Technical Journal of Information Technologies, Mechanics and Optics. 2018. Vol. 18, Issue 2. P. 169–190. doi: <https://doi.org/10.17586/2226-1494-2018-18-2-169-190>
13. MASC – a small Remotely Piloted Aircraft (RPA) for wind energy research / Wildmann N., Hofsäß M., Weimer F., Joos A., Bange J. // Advances in Science and Research. 2014. Vol. 11, Issue 1. P. 55–61. doi: <https://doi.org/10.5194/asr-11-55-2014>
14. Wind Corrections in Flight Path Planning / Selecký M., Váňa P., Rollo M., Meiser T. // International Journal of Advanced Robotic Systems. 2013. Vol. 10, Issue 5. P. 248. doi: <https://doi.org/10.5772/56455>
15. Abufanas A. S., Lobatiy A. A. Bespilotnyy aviacionnyy kompleks kak slozhnaya mul'tistrukturnaya sistema // Sistemniy analiz i prikladnaya informatika. 2015. Issue 1. P. 4–9.
16. Rvachev V. L., Sheiko T. I. R-Functions in Boundary Value Problems in Mechanics // Applied Mechanics Reviews. 1995. Vol. 48, Issue 4. P. 151–188. doi: <https://doi.org/10.1115/1.3005099>
17. Maksimenko-Sheyko K. V. R-funkcii v matematicheskom modelirovanii geometricheskikh ob'ektov i fizicheskikh poley. Kharkiv: IPMash NAN Ukrainy, 2009. 306 p.
18. R-functions in computer modeling of 3D car surface design / Lisin D. A., Maksimenko-Sheyko K. V., Tolok A. V., Sheyko T. I. // Prikladnaya informatika. 2011. Issue 6 (36). P. 78–85.
19. Modelling 3D Steam Turbine Flow Using Thermodynamic Properties of Steam Iapws-95 / Rusanow A. V., Lampart P., Pashchenko N. V., Rusanov R. A. // Polish Maritime Research. 2016. Vol. 23, Issue 1. P. 61–67. doi: <https://doi.org/10.1515/pomr-2016-0009>